Metapopulation dynamics in a complex ecological landscape

E. H. Colombo[1,*] and C. Anteneodo[1,2,†]
[1]*Department of Physics, PUC-Rio, Rio de Janeiro, Brazil*
[2]*Institute of Science and Technology for Complex Systems, Rio de Janeiro, Brazil*
(Received 24 March 2015; published 19 August 2015)

We propose a general model to study the interplay between spatial dispersal and environment spatiotemporal fluctuations in metapopulation dynamics. An ecological landscape of favorable patches is generated like a *Lévy dust*, which allows to build a range of patterns, from dispersed to clustered ones. Locally, the dynamics is driven by a canonical model for the time evolution of the population density, consisting of a logistic expression plus multiplicative noises. Spatial coupling is introduced by means of two spreading mechanisms: diffusion and selective dispersal driven by patch suitability. We focus on the long-time population size as a function of habitat configurations, environment fluctuations, and coupling schemes. We obtain the conditions, that the spatial distribution of favorable patches and the coupling mechanisms must fulfill, to grant population survival. The fundamental phenomenon that we observe is the positive feedback between environment fluctuations and spatial spread preventing extinction.

DOI: 10.1103/PhysRevE.92.022714 PACS number(s): 87.23.Cc, 89.75.Fb, 05.40.−a

I. INTRODUCTION

Habitat fragmentation is commonly observed in nature associated with heterogeneity in the distribution of resources, e.g., water, food, shelter sites, physical factors such as light, temperature, moisture, and any feature able to affect the growth rate of the population of a given species [1]. A fragmented population made of subpopulations receives in the literature the suitable name of *metapopulation* [1–3]. These fragments, also known as patches, are not completely isolated as they are coupled due to movements of individuals in space. For modeling purposes, as a first step one can adopt a single patch viewpoint, taking into account the impact of the surrounding population in an effective manner [4–7]. As a further step beyond the single patch level, one can resort to a spatially explicit model. From this perspective, deterministic and stochastic theoretical models have been developed to obtain the macroscopic behavior of the whole population [2,8–12]. One of the main results is the detection of critical thresholds that delimit the conditions for the sustainability of the population, which occurs for a suitable combination of diverse factors, related to quality and spatial structure of the habitat, migration strategies, and extinction rates. Here, we address related fundamental questions in metapopulation theory proposing a model that includes a general dispersion process, incorporating random and selective dispersal strategies. Additionally, we investigate the model dynamics on top of a complex ecological landscape whose spatial structure can be tuned, ranging from spread to aggregated patches.

In Sec. II, we will describe in detail each part of the model. The spreading process and spatial configuration of the ecological landscape are described in Secs. II A and II B, respectively. The results, reported in Secs. III and IV, focus on the impact of the spatial arrangement of the habitat on its overall viability, that is, on the long-time behavior of the population size. Mainly numerically, and with the aid of analytical considerations, we investigate the impact of habitat topology, spread range, and stochasticity in the long-time behavior of the population size, compared to the corresponding uncoupled metapopulation.

II. MODEL

Let us start from the local dynamics perspective. We assume that the rules that govern the dynamics of a single patch can be primarily modeled by the logistic or Verhulst expression [13] since it mimics reproduction and intraspecific competition which are the two fundamental deterministic driving factors. In mathematical terms, the evolution of the population density (number of individuals per unit area) u_i in each patch i is described by

$$\dot{u}_i = a_i u_i - b u_i^2, \tag{2.1}$$

where a_i and b are real parameters. Such simple model allows to predict the relaxation towards a steady state that can be null ($u_i = 0$) or not ($u_i = a_i/b > 0$), depending on the interplay between the population growth given by the intrinsic growth rate a_i and the intraspecific competition for resources modulated by parameter b.

In real systems, however, the evolution is not deterministic. Stochasticity is introduced mainly by (i) the inherent complexity of the environment, which produces fluctuations in the growth rate (external, environmental noise) and (ii) variations in the birth-death process (internal, demographic noise) [4]. These effects have been previously incorporated to Eq. (2.1) as [4,7,14,15]

$$\dot{u}_i = [a_i + \sigma_\eta \bullet \eta_i(t)]u_i - b u_i^2 + \sigma_\xi \sqrt{u_i} \circ \xi_i(t), \tag{2.2}$$

where σ_η and σ_ξ are positive parameters, and η_i and ξ_i are assumed to be mutually independent zero mean and unit variance Gaussian white noises. The environmental noise term which introduces fluctuations in the growth rate, modulated by σ_η, is expected to have external origins, then, its correlation even if small is non-null, justifying the use of Stratonovich calculus ($\bullet$) to treat its multiplicative nature. The demographic noise, modulated by σ_ξ, represents fluctuations

*eduardo.colombo@fis.puc-rio.br
†celia.fis@puc-rio.br

in the reproduction process of each independent individual, then its magnitude is proportional to the square root of population size, so that its variance is the sum of the variances of independently identically distributed individual stochastic contributions [14,15]. Moreover, under the assumption of uncorrelated and nonanticipative noise, Itô calculus (○) is the adequate choice [4,14–16].

We assume that Eq. (2.2), which is known as canonical model [4,14,15], defines the local dynamics that takes place on each site i of a lattice. Moreover, we will say that a patch i is favorable if it induces positive growth at low densities (i.e., $a_i = A_i^+ > 0$) and unfavorable if it is adverse to support life (i.e., $a_i = A_i^- < 0$).

Spatial coupling is introduced by migrations from one patch to another. Then, the full model can be expressed by

$$\dot{u}_i = a_i u_i - b u_i^2 + D\,\Gamma_i[u] + \sigma_\eta u_i \bullet \eta_i(t) + \sigma_\xi \sqrt{u_i} \circ \xi_i(t), \tag{2.3}$$

where the additional term $D\Gamma_i[u]$, with $D > 0$, is given by the net flux $\Gamma_i[u]$ towards patch i. It is the nonlocal term that couples the set of stochastic differential equations (2.2). We model the populational exchange between patches based on two behavioral strategies: one where the individuals spread in space diffusively, driven by density differences, and another where individuals transit selectively, mainly driven by patch-quality differences. The precise form of these exchanges will be presented in Sec. II A.

Finally, we construct a complex arrangement of favorable and unfavorable patches, that will be defined in Sec. II B. For the sake of simplicity, we consider a binary landscape, where sites can be in any of two states, $A_i^+ = -A_i^- = A > 0$, as assumed in previous studies [17,18]. A typical configuration of the model system in a square lattice is illustrated in Fig. 1.

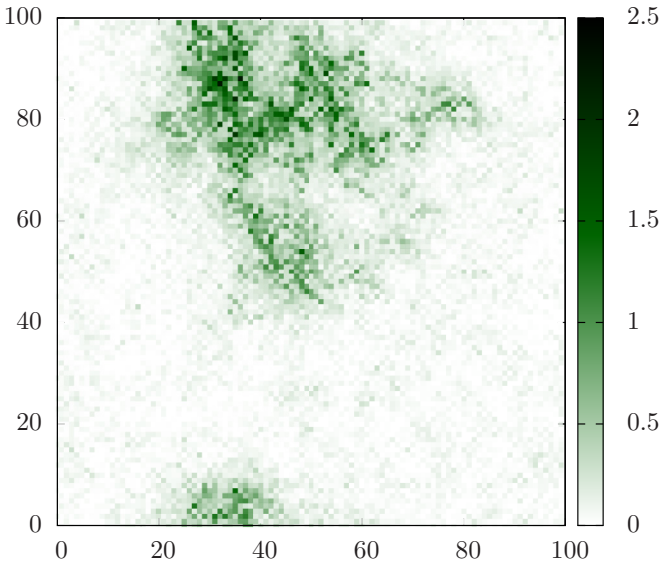

FIG. 1. (Color online) Ecological landscape and population distribution in a square lattice of linear size $L = 100$. Each lattice cell represents a patch. The landscape is defined by the configuration of favorable (positive growth rate) and unfavorable (negative growth rate) patches. A favorable patch is denoted by a black open square. The population density (number of individuals per unit area) is represented by shades of green.

A. Nonlocal coupling

In order to define the coupling scheme, let us state some considerations. First, let us assume that spatial spread is conservative, preserving the number of individuals during travels, and also that it is nonlocal, in the sense that individuals can travel long distances over the landscape, for example, like butterflies and birds [8,19].

Furthermore, it is reasonable to assume that active individuals such as butterflies, birds, and also terrestrial animals use their perception and memory to increase the efficiency in the search for viable habitats. Spatial knowledge can be acquired, for instance, by a direct visualization, previous visit, or by the perception of the collective dynamics. The spatial information stored by the individuals can yield optimized routes between favorable regions. In fact, there is a relation between spatial memory and migration strategy [20]. We introduce this trait by allowing individuals to have access to information about the spatial distribution of patch quality. This will originate selective routes towards favorable patches and some directions will be preferred. Otherwise, if individuals do not have any information about the ecological landscape, or if they do not have memory, uncorrelated trajectories (random movements) can emerge. In fact, this has been the focus of works on animal foraging, where optimal efficiency in resource search occurs without previous knowledge of food distribution [21]. This type of behavior has isotropy as a main trait, indicating directional indifference.

We contemplate both scenarios by modeling spread through a diffusive component together with a contribution of direct routes connecting favorable patches, governed by quality differences. The relative contribution of both mechanisms is regulated by parameter δ, with $0 \leqslant \delta \leqslant 1$ tuning from the ecologically driven ($\delta = 0$) to the purely diffusive ($\delta = 1$) cases. Moreover, we assume that coupling is weighted by a factor $\gamma(d_{ij})$ that decays with the distance d_{ij} [22] between patches i and j, as will be defined in the last paragraph of the current section.

Then, the flux J_{ij} from patch i to j is given by

$$J_{ij} = [\delta + (1-\delta)\alpha_{ij}]\gamma(d_{ij})u_i \geqslant 0, \tag{2.4}$$

where $\alpha_{ij} \equiv (a_j - a_i)/(4A) + 1/2$. Hence, the total flux is

$$\begin{aligned}\Gamma_i[u] &= \sum_{j\neq i}(J_{ji} - J_{ij}) \\ &= \sum_j \gamma(d_{ij})[\delta(u_j - u_i) + (1-\delta)(\alpha_{ji}u_j - \alpha_{ij}u_i)].\end{aligned} \tag{2.5}$$

The total density is conserved by the exchanges described by Eq. (2.5), as can be seen by summing over i. It indicates that individuals tend to move towards patches with fewer individuals and better quality. For $\delta = 1$, Eq. (2.5) represents a generalization of the Fick's law for nonlocal dispersal driven by density gradients. For $\delta = 0$, with our definition of α_{ij}, and binary patch growth rate, the possible values of $\alpha_{ji}u_j - \alpha_{ij}u_i$ are

j \ i	A	$-A$
A	$(u_j - u_i)/2$	u_j
$-A$	$-u_i$	$(u_j - u_i)/2$

This means that, when the quality of two patches is different, the flux occurs in the direction of the higher quality, weighted by the out-flowing population density (lowest quality patch). Only when the quality is the same, diffusive exchange can occur, to allow a network of favorable patches.

Concerning the factor that takes into account the distance between patches, there is empirical evidence [8,23] that the frequency of occurrence of flights between patches decays with the distance, which is reasonable due to the increase of energetic cost. Although diverse decay laws are possible, we will assume exponential decay of the weight γ with the traveled distance ℓ, as observed for some kinds of butterflies [8,23,24], that is,

$$\gamma(\ell) = \mathcal{N}^{-1} \exp(-\ell/\ell_c), \tag{2.6}$$

where ℓ_c is a characteristic length (the average traveled distance) and the normalization constant $\mathcal{N}$ is such that the sum of the contributions of all patches equals one. Operationally, we will truncate the exponential at $\ell \simeq 8\ell_c \ll L$, where L is the linear characteristic size of the landscape.

B. Ecological landscape

In nature, the arrangement of the ecological landscape is built by many distinct processes, occurring in many time scales, creating complex spatiotemporal structures. Then, beyond the inclusion of the environmental noise η, it is also important to take into account the spatial organization of patches [8,9,25,26].

Heterogeneity and patchiness are adequate to capture the complexity of diverse ecological systems [27–31]. Here, we propose to use as complex ecological landscape a *Lévy dust* [21] distribution of favorable patches on a square domain of size $L \times L$ patches, with periodic boundary conditions. Over a background of adverse patches ($a_i = -A$), we construct a Lévy dust of favorable patches ($a_i = A$) given by the sites visited by a Lévy random walk with step lengths ℓ drawn from the probability density function

$$p(\ell) \propto 1/\ell^{\mu}, \tag{2.7}$$

with $1 \leqslant \ell \leqslant L$. This protocol has been used in the study of different problems [21,28,29], but we apply it here in the study of metapopulation dynamics. It allows to mimic a general class of realistic conditions [27,29–31] and to tune different habitat landscapes through parameter μ, from widely spread (for $\mu = 0$) to compactly aggregated in a few clusters separated by large empty spaces (for $\mu = 3$), as illustrated in Fig. 2.

We quantify the change in the spatial structure by computing the probability distribution of the distance d between favorable patches $P_\mu(d)$ (see Fig. 3). For the density $\rho = 0.1$ used in the figure, when $\mu \lesssim 1$, patches are typically far from each other. For high values ($\mu \gtrsim 3$), the generating walk approaches the standard random walk, creating a much more

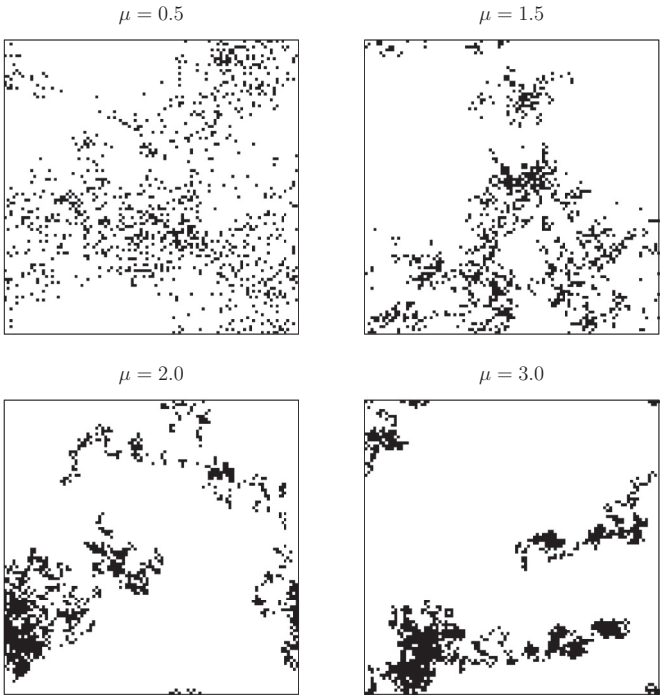

FIG. 2. Ecological landscape for different values of the exponent μ that characterizes the distribution of Lévy jumps given by Eq. (2.7), used to build the configuration of favorable patches in a square domain with $L = 100$. Black cells indicate positive growth rate A (favorable patches) and white cells negative growth $-A$. In all cases, the density of favorable patches is $\rho = 0.1$.

clustered structure, evidenced by the peak at short distances. However, the shape of $P_\mu(d)$ changes with ρ. When the patch density ρ is high, the shape of $P_\mu(d)$ resembles that of the uniform arrangement even for large μ, while at low densities $P_\mu(d)$ presents a peak at small d since the resulting configuration of patches is very localized even for small μ, as will be discussed in Sec. IV C. Furthermore, $P_\mu(d)$ is also sensitive to L, but we kept L fixed ($L = 100$), even if some properties may have not attained the large size limit, as far as μ and ρ allow to scan many qualitatively different possibilities of landscape structure.

C. General considerations about the model

The set of parameters $\{D,\delta,\ell_c\}$ regulate the nonlocal dynamics. While D is the strength of the nonlocal coupling, δ controls the balance between diffusion and directed migration, and ℓ_c defines the coupling range. The ecological landscape is characterized by ρ and μ that set the density and the degree of clusterization, respectively.

In the results presented in the following sections, we will restrict the analysis to a region of parameter space relevant to discuss the main phenomenology of the model. Thus, we will set $A = b = 1$ in all cases. We will also consider $L = 100$ and typically $\rho = 0.1$. Concerning the noise parameters, we set $\sigma_\eta = \sigma_\xi = 0$ to analyze the deterministic case in Sec. III and turn noise on by setting $\sigma_\eta = \sigma_\xi = 1$ in Sec. IV. This choice is based on previous works [4,14]. Indeed, population size can be subject to large fluctuations as demonstrated by experimental data [19].

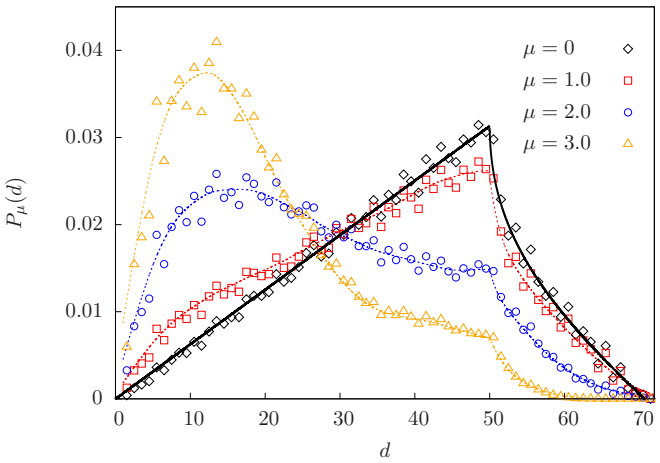

FIG. 3. (Color online) Probability distribution of the distance between favorable patches for different values of exponent μ in Eq. (2.7), for density $\rho = 0.1$ and lattice size $L = 100$ (200 configurations were used). Fluctuations are due to the discrete nature of the possible distances in the lattice. The dotted lines are a guide to the eye. The solid line represents the probability distribution for the distance between uniformly distributed random points in continuous space, drawn for comparison: $P(d) = 2\pi\rho d$ if $d < L/2$, $P(d) = 2\pi\rho d[1 - 4\arccos(L/[2d])]$ otherwise.

We performed numerical simulations of Eq. (2.3) on top of different landscapes, by preparing the system in the stationary state of the deterministic and uncoupled case, i.e., $u_i(0) = \max\{a_i/b,0\}$ for all i, plus a small noise. Integration of Eq. (2.3) was carried out with Euler-Maruyama scheme with a time step $\Delta t = 10^{-3}$. Stratonovich noise was implemented by performing a shift in the drift to obtain the corresponding equivalent Itô version [32].

III. DETERMINISTIC CASE ($\sigma_\eta = \sigma_\xi = 0$)

Before proceeding to study the full model, we consider the deterministic case. Locally, when stochastic contributions are neglected, the asymptotic value of the population size for each patch is $u_i = \max\{a_i/b,0\}$. Introducing nonlocal effects, the population size might change. If population exchanges between patches are guided solely by their quality ($\delta = 0$), then, the favorable-patch network will conserve the initial population size, so no interesting phenomena occur from the viewpoint of extinction. However, when $\delta > 0$, the diffusive behavior induces exploration of the neighborhood independently of habitat quality, which leads to the occupation of unfavorable regions making likely the death of individuals.

By numerical integration of Eq. (2.3) we obtain the time evolution of the total population density $n(t) = \sum_{i=1}^{L^2} u_i(t)$. In Fig. 4, we show the outcomes for fixed values of the model parameters and different initial conditions (different landscapes). While some of the realizations lead to exponential decay of the population, other ones attain finite values at long times. Several different non-null steady states can be attained. Notice, however, that the steady values of different realizations are all below that of the uncoupled case $\rho L^2 A/b = 1000$ for the parameters of the figure. Hence, diffusion favors the decrease of the total population density and the occurrence of extinctions, as expected.

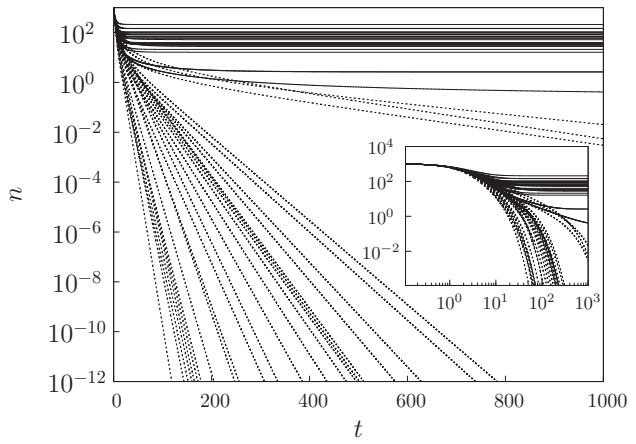

FIG. 4. Deterministic ($\sigma_\eta = \sigma_\xi = 0$) time evolution of the total population density n in different initial landscapes, for $\delta = 1$, $\rho = 0.1$, $D = 10$, $\ell_c = 0.5$, and $\mu = 1.7$. This particular set of values of the parameters results in about half of 50 realizations leading to extinction. We use a dotted line to flag the ones that tend to extinction exponentially fast and a solid line for those that lead to population survival. Alternatively, the same data are represented as a log-log plot in the inset.

In order to investigate how the fraction of survivals changes with the topology, we plot in Fig. 5 the number of survivals per realization f_s as function of the landscape parameter μ, for several values of the coupling coefficient D. Aside from the initial condition used throughout this paper (see Sec. II C), we observed that a perturbation of the null state also leads to the same results of Fig. 5. For given μ, increasing D favors the occurrence of extinctions as already commented above. For given D, below a threshold value of μ the population becomes extinct in all the realizations, while above a second threshold

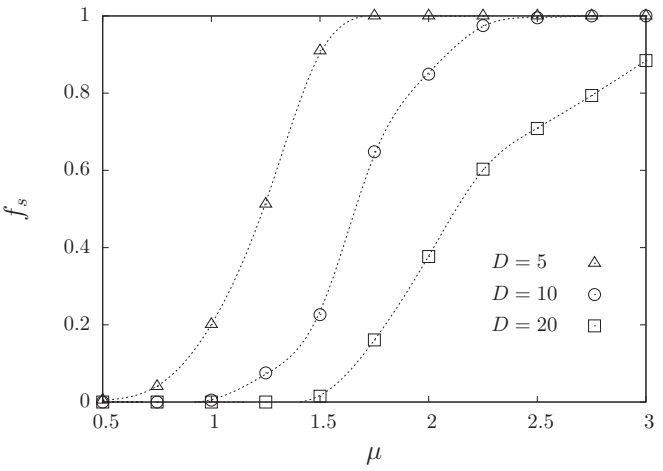

FIG. 5. Fraction of surviving metapopulations f_s (over 100 realizations) in the deterministic case ($\sigma_\eta = \sigma_\xi = 0$) as a function of exponent μ in Eq. (2.7) that gives the degree of clusterization. The other parameters are $\delta = 1$, $\rho = 0.1$, $\ell_c = 0.5$ for the values of the coupling coefficient D indicated on the figure. In this and following figures, dotted lines are a guide to the eye.

it always survives (for the finite number of realizations done), between thresholds both states, the null and non-null ones, are accessible. The number of non-null stable states increases with μ.

Summing over all i the deterministic form of Eq. (2.3), one finds that the steady solution $\dot{n} = 0$ must satisfy $\sum_i a_i u_i = b \sum u_i^2$, which has infinite solutions between the fundamental null state and the uncoupled case solution (the only stable one for $D = 0$). The condition for stationarity of the total density depends only on the local parameters since fluxes are only internal, however, the coupling and landscape can stabilize configurations other than the trivial ones. Furthermore, in the Appendix, we performed an approximate calculation to show that, for small D (recalling that $a_i = \pm A$), the null state is stable if

$$A - D(1 - \gamma_\mu) > 0, \tag{3.1}$$

where $0 \leqslant \gamma_\mu \leqslant 1$ is a factor that mirrors the topology, as defined in Eq. (A3), varying from $\gamma_\mu = \rho$ for the uniform case $\mu = 0$ to $\gamma_\mu = 1$ in the limits of large μ or large ρ. Despite that this approximate expression fails in providing accurate threshold values, it predicts that survival is facilitated by larger A and spoiled by increasing D. It also qualitatively predicts the impact of the topology, as far as it indicates that the destructive role of diffusion can be compensated by a large enough degree of clusterization of the resources given by large γ_μ.

IV. STOCHASTIC CASE

First, let us review some known results about the local (one site) dynamics, which is obtained in the limit $D \to 0$ of Eq. (2.3) (canonical model). In the deterministic case, the two-state habitat [17,18] leads to local extinction (if $a_i = -A$) or finite population (if $a_i = +A$). The presence of stochastic contributions changes the stability of the patches. When $a_i = -A < 0$, the local extinction event predicted deterministically is reinforced by noise. For $a_i = +A > 0$, the demographic (Itô) noise ξ (in the presence of the Stratonovich noise η) leads to extinction in a finite time. But, this time diverges as $\sigma_\xi \to 0$ [4,6]. This divergence is due to the fact that when only the Stratonovich noise η is present, the null state is strictly not accessible, for any noise intensity, in the continuous model. That is, the external noise η reduces the most probable value of the population size, that becomes very close to zero, but non-null, when $\sigma_\eta > \sqrt{2A/b}$ [33].

The population stability can be quantified by the mean time to extinction $\mathcal{T}$ averaged over realizations starting at $u(0)$. For Eq. (2.3) with $D = 0$, $\mathcal{T}$ is given by [14]

$$\mathcal{T} = \int_0^{u_0} \int_z^\infty \frac{\exp\left[\int_z^v \Psi(u)du\right]}{V(v)} dv\, dz, \tag{4.1}$$

where $\Psi(u) = 2M(u)/V(u)$, with $M(u) = au - bu^2 + \sigma_\eta^2 u/2$ and $V(u) = \sigma_\eta^2 u^2 + \sigma_\xi^2 u$. The results of Eq. (4.1) are in good accord with those from numerical simulations, as illustrated in Fig. 6. When the noise intensity decreases, the time to extinction always increases, being divergent in the limit $\sigma_\xi \to 0$.

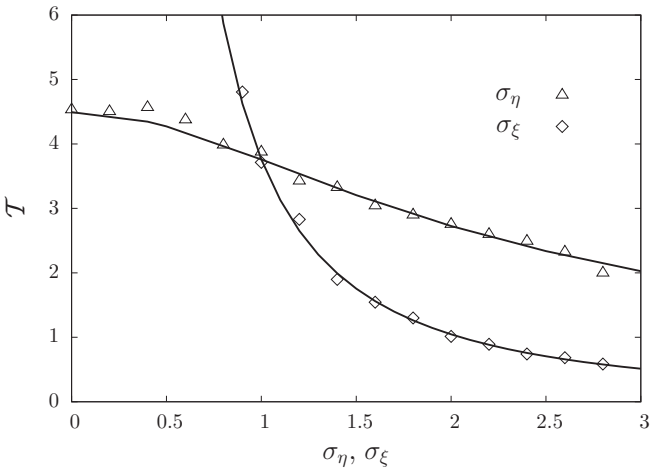

FIG. 6. Single patch dynamics. Mean extinction $\mathcal{T}$ time vs noise strengths σ_η (fixing $\sigma_\xi = 1$, triangles), that modulates the fluctuations in the growth rate, and σ_ξ (fixing $\sigma_\eta = 1$, diamonds), that modulates the demographic noise. Symbols correspond to numerical simulations averaged over 500 samples and the full lines to the theoretical prediction given by Eq. (4.1). The curve for variable σ_ξ diverges in the limit $\sigma_\xi \to 0$.

A. From local to global behavior

In this section, we investigate the effects introduced by patch coupling, i.e., when $D \neq 0$. Nonlocal contributions redistribute the individuals in space, driven by density and quality gradients. In Fig. 7, we show that $D \neq 0$ prevents the extinction events that occur when $D = 0$ (see Fig. 6). Therefore, in contrast to the deterministic case, now spatial coupling is constructive. On the other hand, noise has also a constructive role when $D \neq 0$, differently to the uncoupled case, not only preventing extinction but also contributing to the increase of the population (as in the case $D = 10$). In a

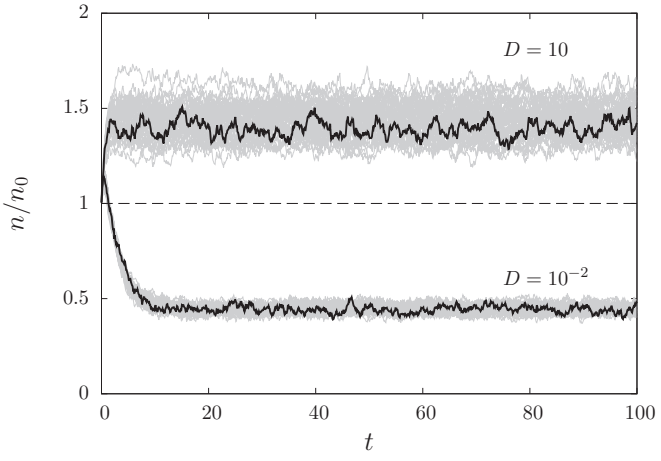

FIG. 7. Temporal evolution of n/n_0, the total population density relative to the initial value n_0 (set as the uncoupled deterministic value). For $\delta = 0.5$, $\rho = 0.1$, $\ell_c = 0.5$, $\mu = 2.0$, $\sigma_\eta = \sigma_\xi = 1$ and values of the coupling coefficient D indicated on the figure. We highlight a single realization (black full line) for each set of 50 realizations (gray lines). The dashed line at $n = n_0$ is plotted for comparison.

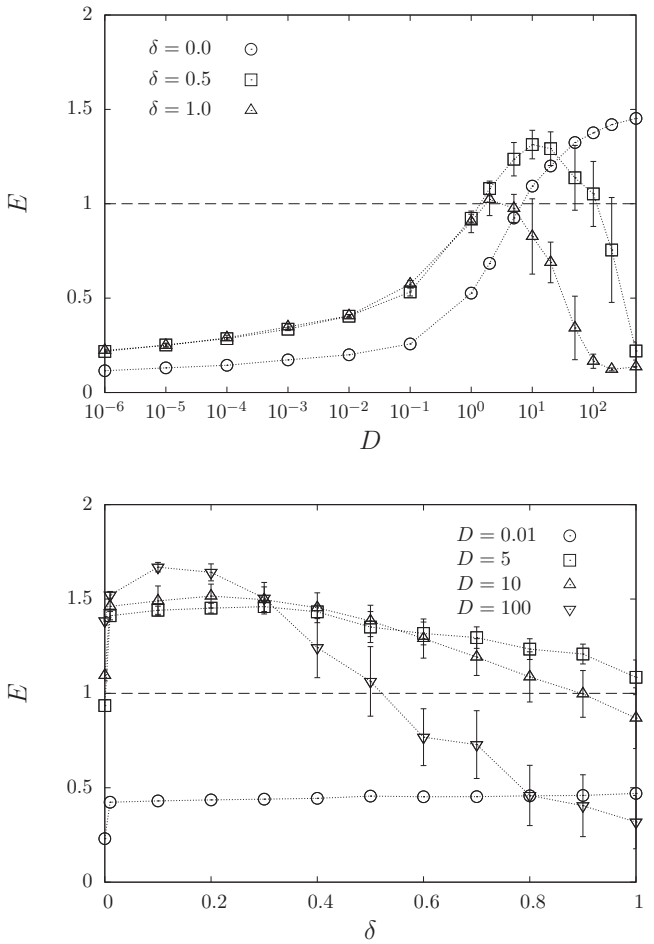

FIG. 8. Long-time relative total population density $E \equiv \langle n_\infty \rangle / n_0$, as a function of the coupling coefficient D, for different values of δ (upper panel) and E as a function of δ, for different values of D (lower panel). Recall that parameter δ regulates the balance between the diffusive ($\delta = 1$) and selective ($\delta = 0$) strategies. The other parameters are $\rho = 0.1$, $\ell_c = 0.5$, $\mu = 2.0$, and $\sigma_\eta = \sigma_\xi = 1$. The symbols represent the average over 20 samples and the vertical bars the standard error. The dashed line at $E = 1$ is plotted for comparison.

previous work [7], we already observed the constructive role in population growth of linearly multiplicative Stratonovich noise in contrast with the destructive behavior of its Itô version. Therefore, environmental noise and coupling have a positive feedback effect on population growth, as shown in Fig. 7.

We will compute the long-time total population density $n_\infty \equiv \lim_{t\to\infty} n(t)$, which is useful to be compared with the initial value $n_0 \equiv n(0) = \rho L^2 u_0 = \rho L^2 (A/b)$, that represents the asymptotic total density in the deterministic uncoupled case. Then, we will measure the long-time relative total population density $E \equiv \langle n_\infty \rangle / n_0$, that represents a kind of efficiency, where the brackets indicate average over landscapes and noise realizations.

In the upper panel of Fig. 8, we plot the long-time relative value E as a function of D. We see that for very small values of D, the population is non-null, although the final relative population density E is smaller than one. Moreover, for given D, the long-time relative value E is smaller when the diffusive component is absent ($\delta = 0$). In all cases, E first increases with D and even exceeds the value $E = 1$, indicating again that not only the noise has a constructive role in preventing extinction, but also in promoting the increase of the initial total population. When the diffusive strategy is present ($\delta > 0$), the increase of E occurs up to an optimal value of the coupling D (with $E > 1$), above which the E decays. Hence, there is a nonlinear effect that does not reflect the linear combination in Eq. (2.4), as shown in the lower panel of Fig. 8. The diffusive component, despite being much less efficient, placing individuals in unfavorable regions, acts with greater connectivity. Then, for small D, the nonlocal contribution of the diffusive coupling is much higher than in the $\delta = 0$ case, leading to a higher population size. In fact, the abrupt transition in the connectivity of the spatial coupling is mirrored in the abrupt change suffered by E as δ becomes non-null. Contrarily, for high values of D, $\delta = 0$ is more efficient due to high damage caused by an intense dispersal towards unfavorable regions, which in the case of Fig. 8 are the majority of the sites. All these observations highlight the importance of the diffusive strategy, that can become more efficient than the ecological pressure driven by the quality gradient.

B. Habitat topology and coupling range

The nonlocal contribution results from the combination of the spread strategies, interaction range, and topology, characterized by δ, ℓ_c, and μ, respectively. Figure 9 shows the long-time relative population density E as function of μ with different values of ℓ_c for $\delta = 1$ and 0.

$E > 1$ means that the combination of habitat topology and spatial coupling range leads the population to profit from the environment fluctuations, increasing its size. The region $E > 1$ is bigger when individuals are selective with respect to their destinations ($\delta = 0$) and increases with ℓ_c. For the diffusive strategy ($\delta = 1$), $E > 1$ is attained only in a clustered habitat (large μ) together with short-range dispersal (small ℓ_c). We have already seen that in a sparse habitat, diffusion represents a waste, especially if the dispersal is long range. Instead, when $\delta = 0$, the habitat does not need to be so clustered or the range so short for population growth. In this instance, the optimal combination occurs in a clustered habitat but with long-range coupling. Finally, note that, as ℓ_c increases, E becomes independent of the topology.

C. Density of favorable patches

Another important issue is the influence of the density ρ of favorable patches in the dynamics. Until now, we have kept it constant to highlight the effects of the heterogeneity of the habitat and of the coupling schemes in the long-time behavior of the total population size. In terms of the protocol used to generate the ecological landscape, ρ not only changes the proportion of favorable patches, but also reshapes the distribution of distances between favorable patches. In Fig. 10, we show three different outcomes of the spatial structure and the corresponding distance distribution for a fixed value of $\mu = 2$. For low ρ, patches organize in a kind of archipelago structure, that is much smaller than the system size, and the distance resembles that obtained for large μ when $\rho = 0.1$.

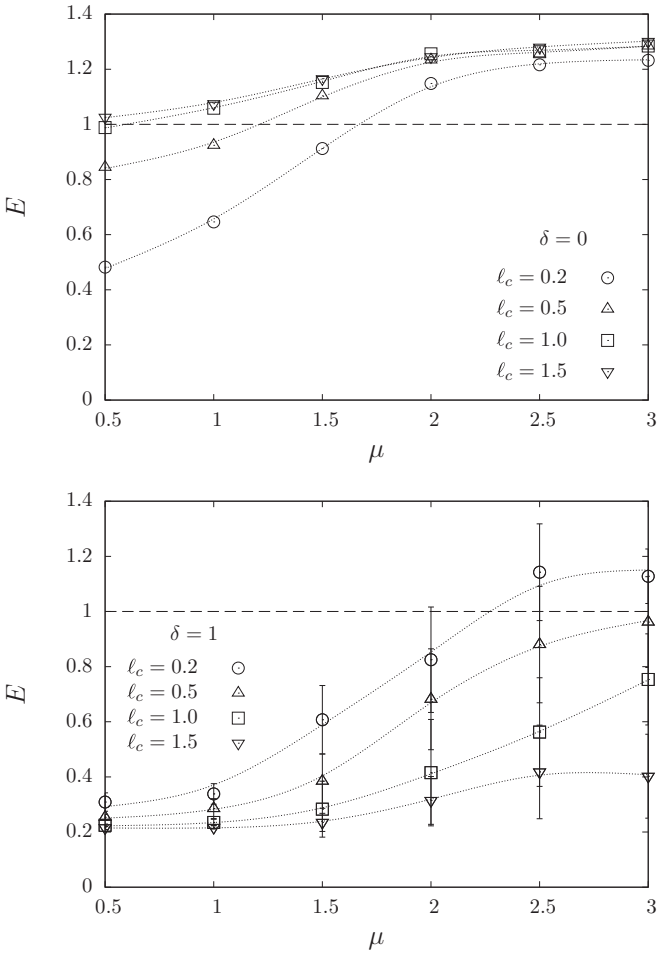

FIG. 9. Long-time relative total population density $E \equiv \langle n_\infty \rangle / n_0$, as a function of exponent μ in Eq. (2.7) for different values of the coupling range ℓ_c, when $\delta = 0$ (selective strategy, upper panel) and $\delta = 1$ (diffusive strategy, lower panel), with $\rho = 0.1$, $D = 20$, and $\sigma_\eta = \sigma_\xi = 1$. The symbols represent the average over 20 samples and the vertical bars the standard error. The dashed line at $E = 1$ is plotted for comparison.

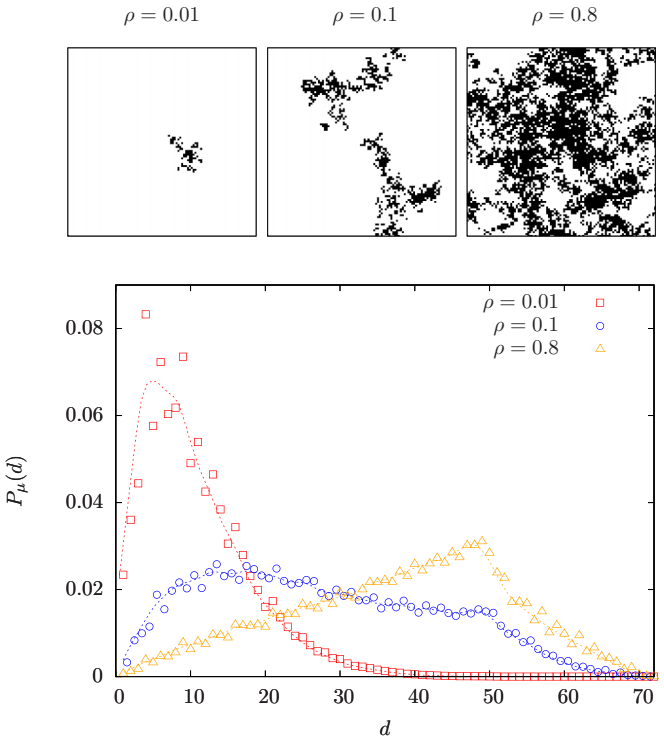

FIG. 10. (Color online) Ecological landscape (upper panels), with favorable patches in black, probability distribution of the distance between favorable patches, averaged over 100 landscapes (lower panel). Three different values of ρ, indicated on the figures, were considered. In all cases, Lévy exponent $\mu = 2$.

For high ρ, many points of the domain are visited creating a distance distribution that approaches the homogeneous form. For μ higher than the value of the figure, profiles very similar to those shown in Fig. 10 are obtained. Meanwhile, for small values of μ, the distribution is almost invariant with ρ, being very close to that of the uniform case. This is due to frequent flights with lengths of the order of system size. Concerning the factor γ_μ that reflects the topology, as defined in Eq. (A3), it can be affected by ρ more through the amount of favorable patches n_v than by its indirect consequences on the spatial distribution P_μ.

In Fig. 11, we show E as a function of ρ for the case $\mu = 2$. By comparing the outcomes for different values of δ, we see the impact of distinct connectivities. In order to interpret this figure, recall that the initial population density n_0 is proportional to the number of favorable patches n_v, namely, $n_0 = n_v A/b = \rho L^2$.

For $\delta = 1$, E presents a minimum value for $\rho \simeq 0.15$. Beyond this value, E grows with ρ attaining the value of the full favorable lattice. In the opposite limit of vanishing ρ (no favorable patches), E diverges as far as, according to the model, (intrinsically) favorable patches are not necessary to promote growth, due to the noisy growth rate. However, if noise is

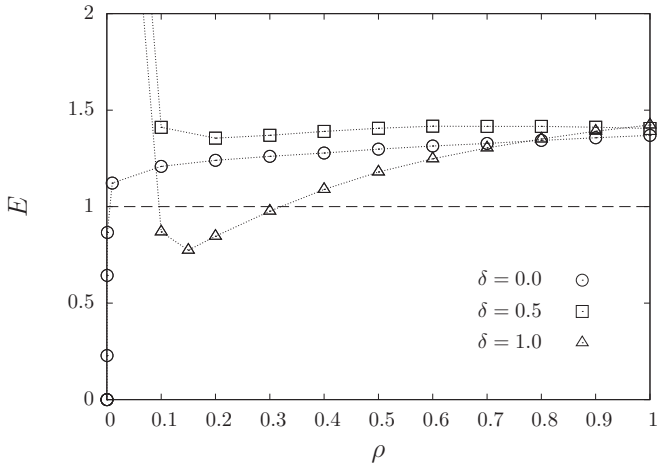

FIG. 11. Long-time relative total population density $E \equiv \langle n_\infty \rangle / n_0$ as a function of the favorable-patch density ρ. Different values of the strategy balance parameter δ were also considered as indicated on the figure. Recall that δ allows to tune from the purely diffusive strategy ($\delta = 1$) to the selective one ($\delta = 0$). The remaining parameters are $A = b = 1$, $D = 20$, $\ell_c = 0.5$, $\mu = 2.0$, $\sigma_\eta = \sigma_\xi = 1$, and $L = 100$. The symbols represent the average over 20 samples and the vertical bars the standard error. The horizontal line represents $E = 1$.

reduced, then the stochastic dynamics approaches the deterministic one, where the population will certainly become extinct.

Now, turning our attention to the $\delta = 0$ case, E is monotonically increasing with ρ, also attaining a limiting value when $\rho \to 1$. Differently from the diffusive case, there exists a critical value $\rho_c = 4 \times 10^{-4}$ ($n_v = 4$) for population survival.

For small ρ, it is curious that the role played by the connectivity, according to the model, makes the diffusive behavior more efficient, while selective moves are important at high values of ρ. In this case, when the system is approaching a fully favorable landscape, the long-time relative population density E tends to be the same for different values of δ. For intermediate values of ρ, we see that the selective strategy overcomes the diffusive one (but never overcomes the combined scheme).

V. CONCLUDING REMARKS

We implemented a general model in which the local dynamics, ruled by the canonical model [14], was coupled through different schemes on top of a complex landscape. This setting allowed to study the role of the habitat spatial structure and the stochastic fluctuations on the long-time state of the metapopulation. We restricted the analysis to a region of parameter space relevant to display the main features and the interplay between the different processes involved. For the deterministic case, we have shown that, for small coupling coefficient D, the distribution of favorable patches must be clustered (large μ) enough for survival, while below a critical value of μ extinction occurs. For the stochastic case, we have shown that noise in combination with spatial coupling has a constructive role, that drives the population to survival, in contrast to the decoupled case where isolated patches would become extinct in finite time. We also studied the effects of the spreading strategy, pointing out that a mixed strategy (diffusive dispersion plus selective routes) will result in a larger population size (Fig. 8).

Furthermore, when the population survives in long-time observations, we analyzed the steady state by means of the quantity $E = \langle n_\infty \rangle / n_0$, which is the quotient between the average long-time population size and its uncoupled deterministic value. This allowed us to highlight the outcome of the combination of spatial coupling and stochasticity, when compared to the case where both are neglected (i.e., $\sigma_\xi = \sigma_\eta = D = 0$). On the one hand, the deterministic dynamics shows that diffusion decreases population size. On the other, in the uncoupled case, stochasticity is responsible to lead population to extinction. Then, both mechanisms when considered separately are harmful to population conservation. However, our results show that the combination of both mechanisms is constructive. This occurs for clustered habitats (large μ). The constructive effect can be enhanced when dispersion is short range (small ℓ_c) under the diffusive strategy, or when dispersion is long range under the selective strategy.

Our model could be improved in several directions, for instance, by considering correlated environment fluctuations, exhaustible resources, etc. But, despite being simple, the model shows the impact of spatial coupling, spatiotemporal fluctuations and their interplay, allowing to foresee the qualitative conditions for population survival as well as the optimal dispersal strategy.

ACKNOWLEDGMENTS

C.A. acknowledges the financial support of Brazilian Research Agencies CNPq and FAPERJ. E.H.C. acknowledges financial support from CNPq and Coordenação de Aperfeiçoamento de Pessoal de Nível Superior (CAPES).

APPENDIX: STABILITY OF DETERMINISTIC STEADY STATES

In order to study how steady state stability is affected by spatial coupling, let us assume that the population is located at the favorable patches, which is true for small D (that is, close to the uncoupled case), and that the coupling is purely diffusive ($\delta = 1$). For a favorable patch, the deterministic form of Eq. (2.3) reads as

$$\begin{aligned} \dot{u}_i &= A u_i - b u_i^2 + D \sum_{j \neq i} (u_j - u_i) \gamma(d_{ij}) \\ &= (A - D) u_i - b u_i^2 + D \sum_{j \neq i} u_j \gamma(d_{ij}), \end{aligned} \tag{A1}$$

recalling that $\sum_{j \neq i} \gamma(d_{ij}) = 1$. To estimate the last term, that represents the flow of individuals from the neighborhood towards patch i, J_i^{in}, we consider that $u_j \approx u_i$. In this case,

$$J_i^{in} = u_i \sum_{j \neq i} \gamma(d_{ij}), \tag{A2}$$

where the sum effectively runs over the n_v favorable patches. The average over arrangements of a landscape $\gamma_\mu \equiv \langle \sum_{j \neq i} \gamma(d_{ij}) \rangle$ can be estimated as

$$\gamma_\mu = n_v \int P_\mu(\ell) e^{-\ell/\ell_c} d\ell. \tag{A3}$$

It depends on μ and on the density ρ, such that it varies from ρ (when $\mu = 0$) to 1, in the extreme cases of either maximal density or very large μ. That is, γ_μ increases with μ, with ρ and with ℓ_c too. Then, Eq. (A1) can be approximated by

$$\dot{u}_i \simeq (A - D[1 - \gamma_\mu]) u_i - b u_i^2 \equiv G u_i - b u_i^2. \tag{A4}$$

If $G > 0$, the population will grow and assume a finite value, bounded by the carrying capacity. Meanwhile, D diminishes the effective growth rate G, that becomes negative for sufficiently large D, namely for

$$D > A/(1 - \gamma_\mu), \tag{A5}$$

indicating decrease of the population. In fact, notice in Fig. 5 that the smaller D the less frequent the extinction events for a given μ. This effect can be mitigated by the landscape, through parameter γ_μ, when the density of favorable sites or clusterization associated with large μ increases. Equation (A5) also provides the linear stability condition for the null state. If $G < 0$, the population will decrease and become extinct.

[1] I. Hanski and I. A. Hanski, *Metapopulation Ecology*, Vol. 312 (Oxford University Press, Oxford, 1999).
[2] I. Hanski, Nature (London) **396**, 41 (1998).
[3] R. Levins, Bull. ESA **15**, 237 (1969).
[4] O. Ovaskainen and B. Meerson, Trends Ecol. Evol. **25**, 643 (2010).
[5] P. A. Hambäck and G. Englund, Ecol. Lett. **8**, 1057 (2005).
[6] B. Meerson and O. Ovaskainen, Phys. Rev. E **88**, 012124 (2013).
[7] L. A. da Silva, E. H. Colombo, and C. Anteneodo, Phys. Rev. E **90**, 012813 (2014).
[8] I. Hanski, M. Kuussaari, and M. Nieminen, Ecology **75**, 747 (1994).
[9] I. Hanski and O. Ovaskainen, Nature (London) **404**, 755 (2000).
[10] S. J. Cornell and O. Ovaskainen, Theor. Populat. Biol. **74**, 209 (2008).
[11] A. North and O. Ovaskainen, Oikos **116**, 1106 (2007).
[12] O. Ovaskainen, D. Finkelshtein, O. Kutoviy, S. Cornell, B. Bolker, and Y. Kondratiev, Theor. Ecol. **7**, 101 (2014).
[13] P. F. Verhulst, Correspondance Mathématique et Physique **10**, 113 (1838).
[14] H. Hakoyama and Y. Iwasa, J. Theor. Biol. **232**, 203 (2005).
[15] H. Hakoyama and Y. Iwasa, J. Theor. Biol. **204**, 337 (2000).
[16] N. Kampen, J. Stat. Phys. **24**, 175 (1981).
[17] C. R. Fonseca, R. M. Coutinho, F. Azevedo, J. M. Berbert, G. Corso, and R. A. Kraenkel, PLoS ONE **8**, e66806 (2013).
[18] R. Kraenkel and D. P. da Silva, Phys. A (Amsterdam) **389**, 60 (2010).
[19] T. H. Keitt and H. E. Stanley, Nature (London) **393**, 257 (1998).
[20] J. M. Berbert and W. F. Fagan, Ecol. Complexity **12**, 1 (2012).
[21] A. Ferreira, E. Raposo, G. Viswanathan, and M. da Luz, Phys. A (Amsterdam) **391**, 3234 (2012).
[22] Given that the boundary conditions are periodic, distances obey the so called minimum image convention. See M. P. Allen and D. J. Tildesley, *Computer Simulation of Liquids* (Oxford University Press, Oxford, 1989). Distances are measured in unit cell side length.
[23] M. Baguette, Ecography **26**, 153 (2003).
[24] Z. Fric and M. Konvicka, Basic Appl. Ecol. **8**, 377 (2007).
[25] L. J. Gilarranz and J. Bascompte, J. Theor. Biol. **297**, 11 (2012).
[26] J. Bascompte and R. V. Sole, J. Anim. Ecol. **65**, 465 (1996).
[27] R. T. Forman, Landscape Ecol. **10**, 133 (1995).
[28] O. Miramontes, D. Boyer, and F. Bartumeus, PLoS ONE **7**, e34317 (2012).
[29] N. Kenkel and D. Walker, Abstracta Botanica **17**, 53 (1993).
[30] G. Sugihara and R. M. May, Trends Ecol. Evol. **5**, 79 (1990).
[31] A. Tsuda, J. Oceanography **51**, 261 (1995).
[32] J. García-Ojalvo and J. Sancho, *Noise in Spatially Extended Systems* (Springer, Berlin, 2012).
[33] W. Horsthemke and R. Lefever, *Noise-Induced Transitions: Theory and Applications in Physics, Chemistry, and Biology* (Springer, Berlin, 2006).